

# Influence of Gas Density Fluctuations on Frequency Stability of Gas Lasers

The statistical fluctuations of gas density within a gas laser cavity change the optical length of the resonator and lead to deformation and lateral displacement of the optical axis. The frequency spread caused by these effects is calculated for typical configurations. It is shown that the main source of frequency instability are the air gaps between the laser tube and the mirrors; the statistical fluctuations within the plasma column are of minor importance. The magnitude of the effect depends on resonator geometry; the effect may markedly deteriorate the final attainable frequency stability of an ultra-stable laser generator. The developed theoretical approach is next used to estimate the influence of acoustic interference. It is found that it also may introduce marked frequency instability. Methods for suppressing the discussed frequency fluctuations are suggested.

## 1. Introduction

With the recent advances in gas laser frequency stabilization by means of saturated absorption techniques the problem of ultimate stability of laser frequency has gained renewed importance. The factors causing frequency instability may be divided into two groups. The first one comprises the effects such as electromagnetic interference, vibrations, thermal drifts etc. which by proper construction or shielding can in principle be eliminated.

To the second group belong the statistical effects of fundamental nature which — at least by present-day techniques — cannot be suppressed. As a consequence, these phenomena determine the ultimate limit of frequency stability. The first one of such effects is the presence of residual spontaneous emission ([1], eq. 17) which is responsible for a frequency spread

$$\Delta f_{sp} \approx (2\pi hf/P) (\Delta f_c)^2.$$

Here,  $f$  and  $P$  is laser frequency and output power, respectively,  $h$  — the Planck constant,  $\Delta f_c$  — the full width of the cavity resonance at its half-points. The frequency spread  $\Delta f_{sp}$  is very small; for instance for a He—Ne laser  $\Delta f_{sp}$  is typically of the order of ( $10^{-3}$  —  $10^{-2}$ ) Hz. Another factor of fundamental character is the frequency spread  $\Delta f_{th}$  due to the thermal vibrations of cavity spacers ([2], eq. 7); typically,  $\Delta f_{th}$  is of the order of a few Hz.

\* Institute of Telecommunication and Acoustics, Technical University of Wrocław, Wrocław, Wybrzeże Wyspiańskiego 27, Poland.

The present paper is devoted to the discussion of another factor of fundamental character which is connected with the statistical fluctuations of gas density. It is shown that this effect can exhibit a marked influence on the ultimate frequency stability of gas lasers. The developed theoretical approach may also be applied to the discussion of acoustic interference. It is found that the respective effects can be a source of considerable frequency instability of gas lasers.

## 2. The Statistical Fluctuations of Position and Tilt of the Equiphasic Surfaces

### 2.1. THEORY

The dependence of the refractive index  $n$  of a gas on its density is given by

$$n = 1 + (n_0 - 1) (\nu/\nu_0), \quad (1)$$

where  $\nu$  and  $\nu_0$  is the concentration of gas molecules at considered and standard conditions, respectively, and  $n_0$  is the refractive index corresponding to the standard concentration  $\nu_0$ . The standard conditions assumed in the present investigation are

$$p_0 = 760 \text{ Tr}; T_0 = 273.15 \text{ K}. \quad (2)$$

The optical path length  $l$  of a ray path of a geometrical length  $L$  in a medium of a refractive index  $n$  is  $l = nL$ . The change of the optical path length due to a change in molecular concentration is thus

$$\Delta l = \frac{n_0 - 1}{v_0} L \Delta v. \quad (3)$$

Eq. (3) will be applied to a light beam of a small cross-section  $S$  and a geometrical length  $L$ . The total number of gas molecules contained within the beam volume  $LS$  is  $N = LSv$ ; hence

$$\Delta l = \frac{n_0 - 1}{v_0} \frac{\Delta N}{S}. \quad (4)$$

Due to the gas density fluctuations the optical path lengths of the rays constituting the laser beam change in a random manner. As a consequence the equiphase surfaces of the beam are deformed and displaced according to the instantaneous distribution of  $\Delta l$  across the considered cross-section of the laser beam. For the purpose of the present analysis it is sufficient to calculate the displacement and deformation of the equiphase surface at the end of the beam travel through the whole length of the considered gaseous medium only. Considering this effect we shall assume for simplicity that the rays of the beam are parallel to the optical axis of the cavity. In order to describe the distribution of  $\Delta l$  across the beam cross-section a coordinate system  $x, y, z$  will be introduced with the  $z$ -axis directed along the symmetry axis of the cavity;  $\Delta l$  will thus be certain random function of coordinates  $x, y$  and time  $t$ . At a given moment  $t$  the displacement  $\Delta l$  will be a function of  $x$  and  $y$  only. This function may be expanded in series around the point  $(0,0)$

$$\begin{aligned} \Delta l(x, y) = & \Delta l_0 + \left( \frac{\partial}{\partial x} \Delta l \right)_0 x + \left( \frac{\partial}{\partial y} \Delta l \right)_0 y + \\ & + \frac{1}{2} \left( \frac{\partial^2}{\partial x^2} \Delta l \right)_0 x^2 + \left( \frac{\partial^2}{\partial x \partial y} \Delta l \right)_0 xy + \\ & + \frac{1}{2} \left( \frac{\partial^2}{\partial y^2} \Delta l \right)_0 y^2 + \dots \quad (5) \end{aligned}$$

The series (5) is a random function of time. The rapidity of the changes of this function depends on the length of the time span during which the considered gas density inhomogeneities form or decay. The shortest length of such time intervals ( $\Delta t_{\min}$ ) may be estimated as a ratio of laser beam diameter to sound velocity. We thus are faced by a problem of a dynamic behaviour of a gas laser similar to that discussed by UCHIDA [3]. Considering loss modulation Uchida found that at high power levels the amplitude variation had a cutoff frequency  $f/(2Q)$  where  $Q$  was the figure of merit of the laser cavity. It is thus necessary to compare  $\Delta t_{\min}$  with  $2Q/f$ . Two typical examples may best clear the situation. As the first example we shall consider a  $\text{CO}_2$  laser

with a cavity 0.5 m long with an effective single pass loss factor of 2.5%; in such case  $2Q/f \approx 0.8 \mu\text{s}$  and  $\Delta t_{\min} \approx 2 \mu\text{s}$  or  $\approx 4 \mu\text{s}$  depending on whether we consider the comparatively light  $\text{CO}_2\text{—N}_2\text{—He}$  mixture inside the tube or the air section contained in the interspace between the laser tube and the cavity mirror. As the second example we shall consider a single-mode  $\text{He—Ne—}0.63 \mu\text{m}$  laser with a cavity 0.1 m long with a single pass loss factor of 0.75%; we then find  $2Q/f \approx 0.6 \mu\text{s}$  and  $\Delta t_{\min} \approx 0.15 \mu\text{s}$  for the  $\text{He—Ne}$  tube fill and  $\approx 0.5 \mu\text{s}$  for the air column. We thus see that in the case of a  $\text{CO}_2$  laser the optical field will easily adjust itself even to the most rapid variations of gas density. In the case of a short single-mode  $\text{He—Ne}$  laser the optical field will follow the slow changes of gas density but may show some lag when the fluctuations are very rapid. However, as may be shown, rapid density fluctuations are relatively seldom. Moreover, as we shall see later, the main source of perturbation are the air columns and not the rarefied gas inside the laser tube.

The above examples are representative of the situation. They show that it is admissible to consider the problem as quasi-stationary i. e. to assume that the optical field corresponds to the actual distribution of the refractive index throughout the cavity. The described situation determines also the averaging time intervals  $\Delta t_{\text{av}}$  for which the mean values of the frequency scatter calculated in the present investigation are valid:

$$\Delta t_{\text{av}} \gg \Delta t_{\min}.$$

The first term of the series (5) represents the change of the optical length of the cavity. This leads to a corresponding change of laser frequency

$$\frac{(\Delta f)_l}{f} = - \frac{\Delta l_0}{D}, \quad (6)$$

where  $D$  is the cavity length. This frequency change may be called the *longitudinal effect*. We shall denote it by the subscript  $l$ .

The second and the third terms of the series (5) describe the relative *tilt* of the equiphase surface at one end of the optical path as compared with the orientation of the wave front at the other end of the path. As a consequence of this effect the optical axis will no longer be a straight line but will be bent transversally. The shape of the deformed optical axis depends on how the changes of the molecule number are distributed along the cavity length. It may be easily shown that the uniform distribution is the most probable one. In such a case also the bending of the optical axis would be uniform i. e.

the optical axis would take the shape of an arc. The probability of a markedly non-uniform distribution is small or even very small. Moreover, the non-uniform bending of the axis produces similar effects as that found in the case of a uniform effect. This is especially true when considering the practically most important influence of the air sections of the laser cavity. In view of the purpose and character of the present investigation it seemed admissible to assume that bending is uniform, i. e. that the optical axis is deformed into an arc.

The perturbed optical field must satisfy the boundary conditions at the cavity mirrors. As a consequence, in the cases when the curvature of the wavefronts remains unchanged and only longitudinal effect and transverse bending are effective the bent optical axis must move so as to be again normal to both mirrors. The equiphase surfaces of the deformed field will then in a due manner coincide with mirror surfaces at both ends. For a laser with internal mirrors the situation is then as shown in Fig. 1 with the bent optical axis  $B_1B_2$  displaced side-ways.

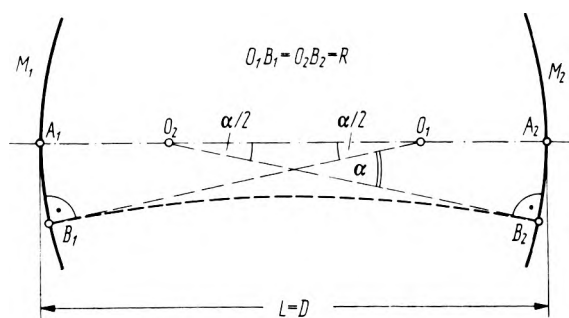


Fig. 1. Displacement and deformation of the optical axis in the case of a laser with internal mirrors;  $O_1, O_2$  — centres of curvature of mirrors  $M_1, M_2$

The length of the gas column  $L$  which must be taken into account when computing  $\Delta l$  is then equal to the cavity length  $D$ . In the case of a laser with external mirrors the total bending — as will be shown later — occurs practically within the air gaps. Fig. 2 illustrates the influence of one air section; the deformed optical axis  $B_1O_2B_2$  moves then side-ways and bends. In such a case  $L < D$  or even  $L \ll D$ .

The length of the deformed optical axis in its new position is different from that when the undisturbed axis was a straight line. Then the laser frequency changes accordingly. This change may be called the *transverse effect*. We shall denote it by the subscript  $t$ .

In the case of both the longitudinal and the transverse effect the change in frequency is caused by the variation of the effective length of the optical axis within an *unchanged* cavity. Quite different

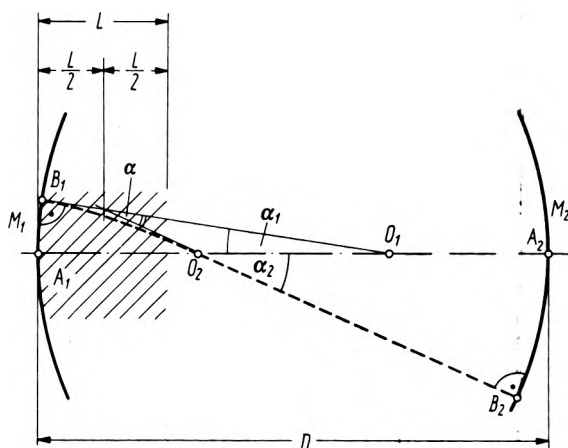


Fig. 2. Displacement and deformation of the optical axis caused by one air gap (schematically)  
The air gap shown shaded.  $O_1, O_2$  — centres of curvature of mirrors  $M_1, M_2$

phenomena are connected with the higher order terms of the series expansion (5). In general, they are equivalent to the aspherical deformations of the laser mirror surfaces. This presents a mathematical problem of a completely different character as compared with the previous one; we shall not discuss it in the present paper. As a consequence we shall disregard the higher order terms of the series (5) and shall assume that the relative displacement of the equiphase surfaces is described by the first three linear terms only

$$\Delta l(x, y) = \Delta l_0 + a_x x + a_y y. \quad (7)$$

Eq. (7) represents a plane displaced and inclined with respect to the  $x, y$ -plane; this perturbation plane we shall call the  $P$ -plane. The point at which the  $P$ -plane cuts the  $z$ -axis determines the value of  $\Delta l_0$ . The tilt of the  $P$ -plane is calculated as a small angle  $\alpha$  between the normal to the  $P$ -plane and the  $z$ -axis. The angle  $\alpha$  is at the same time the total angle by which the optical axis is bent (compare Figs. 1 and 2).

In order to determine the position of the  $P$ -plane it is sufficient to calculate the value of  $\Delta l$  at three non-colinear points. These three points must be chosen to be representative of the gas density inhomogeneity. To this purpose we shall divide the total cross-section  $S_t = \pi r^2$  of the laser beam into three equal segments of the same cross-sections  $S_s = \frac{1}{3} S_t$  (Fig. 3). The three representative points we choose as the gravity centres of the segments. They then lie at the distance  $\rho = (\sqrt{3}/\pi)r$  from the origin. The cross-sections  $S_s$  of the segments will be substituted for  $S$  in eq. (4). Consequently,  $N$  from eq. (4)

will now mean the total number of gas molecules contained within the partial volume  $LS_i$  of the segments 1, 2, 3; we shall denote it by  $N_{si}$  ( $i = 1, 2, 3$ ).

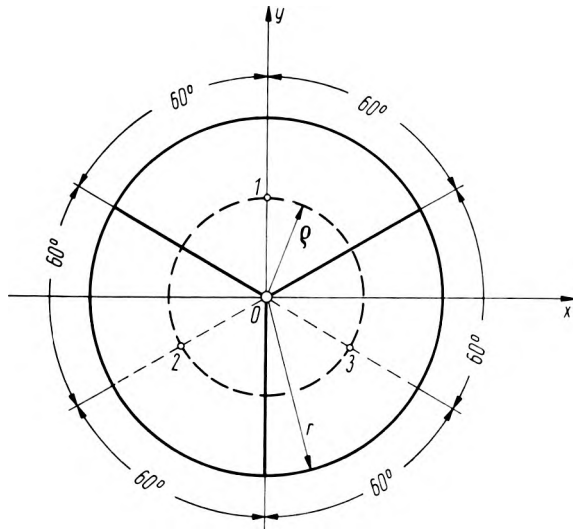


Fig. 3. Division of the laser beam cross-section into three segments;  $r$  - beam radius

The displacements  $\Delta l_i$  at the points 1, 2, 3 in Fig. 3 are then

$$\Delta l_i = 3 \frac{n_0 - 1}{v_0 S_i} \Delta N_{si}, \quad (i = 1, 2, 3). \quad (8)$$

The value of  $\Delta l_0$  we find as the arithmetic mean of all  $\Delta l_i$

$$\Delta l_0 = \frac{n_0 - 1}{v_0 S_t} \Delta N_t, \quad (9)$$

where  $N_t = N_{s1} + N_{s2} + N_{s3}$  is the total number of gas molecules contained within the entire considered beam region of the length  $L$  and the full cross-section  $S_t$ .

Computation of the bending angle  $\alpha$  is simplified due to the smallness of  $\alpha$ . We finally obtain

$$\alpha = \frac{n_0 - 1}{v_0} \frac{2}{\sqrt{3} r^3} \times [(\Delta N_{s1})^2 + (\Delta N_{s2})^2 + (\Delta N_{s3})^2 - \Delta N_{s1} \cdot \Delta N_{s2} - \Delta N_{s2} \cdot \Delta N_{s3} - \Delta N_{s3} \cdot \Delta N_{s1}]^{1/2}. \quad (10)$$

Because of the statistical character of the phenomena it is necessary to determine the scatter of  $\Delta l_0$  and  $\alpha$ . Assuming that a particle is equally like to arrive at any time, i. e. that the particles are statistically independent, the standard deviation of the molecule number  $\sigma(N)$  for large  $N$  is given by ([4], eq. 5.19; [5], eq. 48)

$$\sigma(N) = (\bar{N})^{1/2}, \quad (11)$$

where  $\bar{N}$  is the mean of  $N$ . For  $\Delta l_0$  we thus find

$$\sigma(\Delta l_0) = \frac{n_0 - 1}{v_0 S_t} (\bar{N}_t)^{1/2}. \quad (12)$$

The average number of molecules contained within a gas column of the volume  $S_t L$  is

$$N_t = L S_t v_0 \frac{p}{p_0} \frac{T_0}{T}, \quad (13)$$

where  $p$  and  $T$  are pressure and absolute temperature of the gas, and  $p_0$ ,  $T_0$  are the standard values. Substituting from (13) into (12) we find

$$\sigma(\Delta l_0) = \frac{n_0 - 1}{\sqrt{\pi} v_0} \sqrt{\frac{p}{p_0} \frac{T_0}{T} \frac{V L}{r}}. \quad (14)$$

When calculating  $\sigma(\alpha)$  we start from the definition of the standard deviation  $\sigma(\alpha) = (\overline{\alpha^2})^{1/2}$  and obtain

$$\sigma(\alpha) = \frac{n_0 - 1}{v_0} \frac{2}{\sqrt{3} r^3} \times [(\overline{\Delta N_{s1}^2}) + (\overline{\Delta N_{s2}^2}) + (\overline{\Delta N_{s3}^2}) - (\overline{\Delta N_{s1} \cdot \Delta N_{s2}}) - (\overline{\Delta N_{s2} \cdot \Delta N_{s3}}) - (\overline{\Delta N_{s3} \cdot \Delta N_{s1}})]^{1/2}.$$

According to eq. (11)  $\overline{\Delta N_{si}^2} = \bar{N}_{si}$ . As regards the product terms the random numbers  $N_{si}$  are statistically independent; we then have ([4], eq. 5.20)

$$(\overline{\Delta N_{s1} \cdot \Delta N_{s2}}) = 0,$$

and similarly for the remaining product terms. As a consequence

$$\begin{aligned} \sigma(\alpha) &= \frac{n_0 - 1}{v_0} \frac{2}{\sqrt{3} r^3} \sqrt{\bar{N}_t} \\ &= (n_0 - 1) \sqrt{\frac{4\pi}{3v_0}} \sqrt{\frac{p}{p_0} \frac{T_0}{T} \frac{V L}{r^2}}. \end{aligned} \quad (15)$$

In the case when it is necessary to compute the influence of a number of different gas sections  $L_1$ ,  $L_2$  etc. the effect for each one can be evaluated independently and the final result calculated according to the rules of statistic of independent random phenomena.

## 2.2. THE EFFECTIVE BEAM RADIUS AND THE REFRACTIVE INDEX OF THE GASEOUS MEDIUM

The diameter of the laser beam is not constant along its way through thy cavity. In the case of a symmetrical cavity of length  $D$  equipped with mirrors of equal radii  $R$  the radii of the beam at its waist ( $w_0$ ) and in the mirror planes ( $w_m$ ) are given by [6]

$$w_0 = \sqrt{\frac{\lambda}{2\pi} \sqrt{D(2R-D)}}, \quad (16)$$

$$w_m = \sqrt{\frac{\lambda}{\pi} \frac{RV D}{\sqrt{2R-D}}} \quad (17)$$

When considering the influence of a plasma section we may take as an effective beam radius  $r$  the geometric mean of  $w_0$  and  $w_m$

$$r = \sqrt{w_0 w_m} = \sqrt{\frac{\lambda}{\pi} \sqrt{\frac{1}{2} RD}} \quad (18)$$

When considering the influence of the air gap between the laser tube and a mirror we may put

$$r = w_m \quad (19)$$

In the case of an asymmetrical resonator with a plane and a spherical mirror or a cavity with a blazed diffraction grating we can use eq. (16) and (17) except that  $D$  must be replaced by  $2D$ . Beam radius at a plane mirror or a grating is then given by (16) and that at a spherical mirror by (17).

In the general case of an asymmetrical cavity the beam diameters are calculated as explained in [6].

The relation between the refractive index  $n$  of a gas at a pressure  $p$  and an absolute temperature  $T$  and that under standard conditions ( $n_0, p_0, T_0$ ) is given by

$$n-1 = (n_0-1) \frac{pT_0}{p_0T} \quad (20)$$

When calculating the refractive index of the laser plasma a due consideration must be given to the peculiarities of the active medium. The refractive index may then be considered as composed of three constituents.

The first term ( $n'$ ) arises from the densities of ground-state atoms and the excited atoms which may participate in neighbouring transitions. This term is practically constant across the laser transition profile. For a moderately excited gas the ground state population will be orders of magnitude in excess of that of any other state and to a good accuracy the refractive index  $n'$  may be approximated by the value characteristic of the non-excited gas.

The second contribution to the refractive index ( $n''$ ) is connected with the transition responsible for the amplification. This term, as arising from a resonance phenomenon, changes markedly across the laser transition profile. According to Kramers-Kronig relation the additional phase shift  $\Delta\Phi(f)$  at the frequency  $f$  depends on the fractional gain per pass  $g(f)$  and the distance from the line centre  $f_m$ . For a Lorentzian line this relation can easily be evaluated to give (see for instance [7], eq. 2.109)

$$\Delta\Phi(f) = \frac{g(f)(f-f_m)}{(\Delta f)_{\text{line}}}$$

where  $(\Delta f)_{\text{line}}$  is the full width of the line at the half-gain points. Then

$$n''-1 = \frac{c}{2\pi f D} \Delta\Phi(f), \quad (21)$$

where  $c$  is light velocity. This formula may be used as a guide when estimating the effect. In most cases gain is low; besides, for highly stable gas lasers the distance from the line centre ( $f-f_m$ ) is very or extremely small. The contribution to the refractive index is then negligible. However, in the case of an active medium of very large gain and a laser stabilized with reference to an absorption line lying rather far from the centre of the laser transition the term  $n''-1$  may be quite large or even dominant.

The third contribution to the refractive index comes from the electron gas. It is very small and for the present purpose may be completely disregarded.

We thus see that in most cases a good approximation to the refractive index of the active medium is given by the value characteristic of the non-excited gas. This may be exemplified by the measurements of the refractive index of the CO<sub>2</sub> laser plasma given in [8].

### 2.3. MAGNITUDE OF THE EFFECTS

In order to show the magnitude of the effects the results of calculations for some characteristic examples have been summarized in Table 1. As follows from Table 1 the dominant part of the considered effects is connected with the air gaps.

Table 1

Change in optical length and bending of the optical axis due to the density fluctuations within the gas sections

	He-Ne laser <sup>(a)</sup>		CO <sub>2</sub> laser <sup>(b)</sup>	
	plasma section	one air gap	plasma section <sup>(c)</sup>	air gap
$\sigma(\Delta l_0)$ [m]	$4.6 \times 10^{-16}$	$1.6 \times 10^{-14}$	$7.7 \times 10^{-16}$	$5.2 \times 10^{-15}$
$\sigma(\alpha)$ [rd]	$9.0 \times 10^{-12}$	$3.0 \times 10^{-10}$	$2.4 \times 10^{-12}$	$1.4 \times 10^{-11}$

(a) A single-mode He-Ne laser 0.63  $\mu\text{m}$ . Plasma tube: capillary diameter 0.1 cm, capillary length  $L_p = 10$  cm, total gas pressure 4 Tr,  $p_{\text{He}}:p_{\text{Ne}} = 5:1$ , plasma temperature  $T \approx 400\text{K}$ . Cavity length  $D = 14$  cm. Mirrors of equal radii  $R = 40$  cm. Two air gaps of equal lengths  $L_a = 1$  cm.

(b) A low power CO<sub>2</sub> laser. Plasma tube: internal diameter 1.5 cm, length  $L_p = 45$  cm. Total gas pressure 14 Tr,  $p_{\text{CO}_2}:p_{\text{N}_2}:p_{\text{He}} = 10:12:78$ . Plasma temperature  $T \approx 400\text{K}$ . Cavity length  $D = 50$  cm. Mirrors of equal radii  $R = 60$  cm. One air gap of the length  $L_a = 5$  cm.

(c) Because of the large gain of a CO<sub>2</sub> laser [9] the resonant contribution (21) to the refractive index may be considerable. It has been assumed that the laser is tuned to near the line centre and thus  $n'' - 1 \approx 0$ .

### 3. Frequency Spread for a Gas Laser with Internal Mirrors

The frequency spread due to the *longitudinal* effect can be calculated from eq. (6) by replacing differences  $\Delta$  by standard deviations  $\sigma$ ; thus

$$\sigma(f)_l = \frac{f\sigma(\Delta l_0)}{D}. \quad (22)$$

The frequency spread due to the *transverse* effect arises from the fact that the bent and side-ways displaced optical axis (Fig. 1:  $B_1 B_2$ ) has a length slightly different from that in the unperturbed position (Fig. 1: the straight line  $A_1 O_2 O_1 A_2$ ).

When considering this effect it should in principle be taken into account that the displaced optical axis passes now a region of a slightly different refractive index as that along the cavity symmetry axis  $A_1 O_2 O_1 A_2$ . However, as may be shown, this effect is of no practical influence.

Another factor which could also have some influence is a change in wave velocity linked with the curved shape of the wave axis. Estimating by analogy with the frequency differences existing between various transverse modes of a laser cavity these changes in wave velocity may be expected to be completely negligible.

We thus see that in the case of a laser with internal mirrors the only factor determining the transverse effect is the difference  $\Delta D$  between the geometrical lengths of the perturbed and unperturbed optical axes. This difference  $\Delta D$  plays now the role of  $\Delta l_0$  from eq. (6).

We shall consider a symmetrical cavity of a length  $D$  with mirrors of equal radii  $R$ . The perturbed optical axis is an arc of the length  $D_p$  bent by the angle  $\alpha$  (Fig. 1). Simple calculations give

$$\Delta D = D_p - D = -\alpha^2 \left( \frac{R}{4} - \frac{D}{24} \right). \quad (23)$$

Considering mean values we replace  $\overline{\alpha^2}$  by  $\sigma^2(\alpha)$  and find

$$\overline{(\Delta f)_t} = f \left( \frac{R}{4D} - \frac{1}{24} \right) \sigma^2(\alpha). \quad (24)$$

Contrary to the longitudinal effect the transverse effect is in the present case unidirectional, i. e. it always gives an increase in frequency.

In order to show the magnitude of the effects the longitudinal and transverse frequency spreads have been calculated for the same lasers as quoted in Table 1. The results have been summarized in

Table 2. As may be seen from Table 2 in the case of gas lasers with internal mirrors the longitudinal effect is quite small or very small whereas the transverse effect is completely negligible.

Table 2

Frequency spread due to the longitudinal and transverse effect for gas lasers with internal mirrors

Laser	Transverse effect		Longitudinal effect	
	$\overline{(\Delta f)_t}$ [Hz]	$\overline{(\Delta f)_t}/f$	$\sigma(f)_l$ [Hz]	$\sigma(f)_l/f$
He-Ne	$3.6 \times 10^{-8}$	$7.7 \times 10^{-23}$	1.8	$3.9 \times 10^{-15}$
CO <sub>2</sub>	$4.8 \times 10^{-11}$	$1.7 \times 10^{-24}$	$4.6 \times 10^{-2}$	$1.6 \times 10^{-15}$

The same lasers as in Table 1 except that the lengths of the plasma sections  $L_p$  are now equal to the cavity length  $D$ .

### 4. Frequency Spread in the Case of a Gas Laser with External Mirrors

In the case of a gas laser with external mirrors the frequency fluctuations are due to gas density fluctuations both inside the plasma column and within the air gaps between the laser tube and the cavity reflectors. These different sources of disturbance are statistically independent; we may thus consider each one independently of the other or others. The disturbances created within the plasma and air sections are of different magnitude: as follows from Table 1 the influence of the air sections is dominant. Taking all this into account we shall consider only one air gap as the source of frequency fluctuations. The rest of the optical path will be assumed for the present purpose to be composed of sections of constant refractive index.

Similarly as in the case of a laser with internal mirrors also in the present case we have a longitudinal and a transverse effect. The mechanism of the *longitudinal* effect is the same as described by eq. (22). The frequency spread due to this effect for the lasers from Table 1 has been given in Table 3.

Table 3

Total longitudinal frequency spread connected with the presence of the air gaps

Laser	$\sigma(f)_l$ [Hz]	$\sigma(f)_l/f$
He-Ne	76	$1.6 \times 10^{-13}$
CO <sub>2</sub>	0.3	$1.0 \times 10^{-14}$

The same lasers as in Table 1. For the He-Ne laser the total effect due to both air gaps has been given.

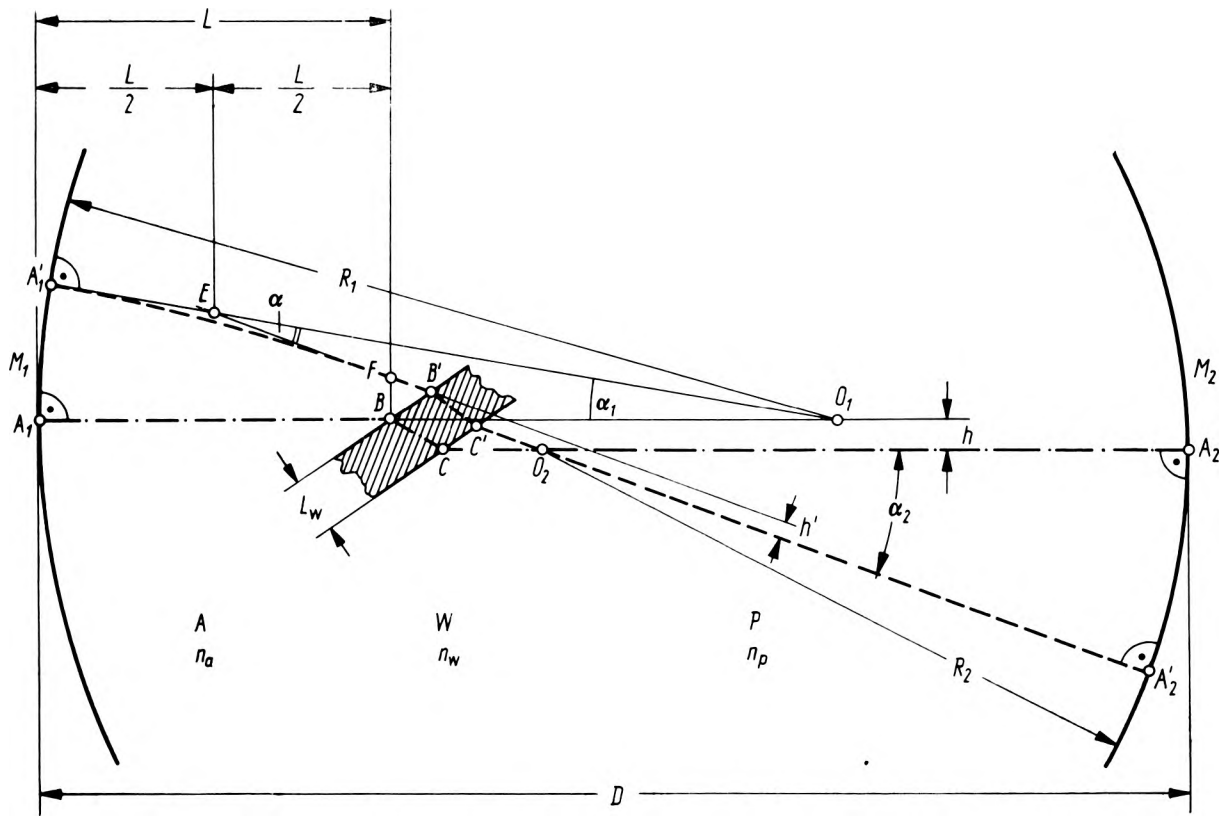


Fig. 4. The shape and position of the unperturbed and perturbed optical axes in the case of a laser with one internal and one external mirror

$M_1, M_2$  – mirrors of the radii  $R_1, R_2$ ;  $O_1, O_2$  – centres of curvature of mirrors  $M_1, M_2$ ;  $A$  – air section;  $W$  – optical window;  $P$  – plasma section;  $n_a, n_w, n_p$  – refractive indices of air, window material and plasma

In the case of external mirrors the calculations of the *transverse* effect are complicated to a surprising degree due to the presence of the Brewster angle windows. As a consequence of the deflection of the optical axis not only change the lengths of all path sections inside the cavity but also varies the lateral parallel displacement  $h$  suffered by the beam on traversing a plane-parallel Brewster window (Fig. 4:  $h' \neq h$ ). On hand of an example of a laser with one internal and one external mirror from Fig. 4 we shall sketch the method of calculation. The unperturbed optical axis runs through points  $A_1BCO_2A_2$ , the perturbed – through  $A'_1FB'C'O_2A'_2$ . The perturbed axis is bent along its air section by the angle  $\alpha$  and displaced from its original position so as to be again perpendicular to both mirrors. The position of the perturbed optical axis is determined by the angles  $\alpha_1$  and  $\alpha_2$  such that  $\alpha_2 - \alpha_1 = \alpha$  and by the magnitude of the lateral displacement  $h' \neq h$ . It is thus necessary to calculate  $\alpha_1, \alpha_2$  and  $h' - h$  in relation to  $\alpha$  and then to compute the changes of optical path lengths for all cavity sections. When considering the final frequency scatter we must take into account that only deflection in the plane of Fig. 4 gives first order

effects. Deflection perpendicular to that plane produces second order effects only which may be disregarded completely. It is thus necessary to consider the deflection components in the plane of Fig. 4 only. To account for it in the final formulae for frequency scatter a factor  $1/\sqrt{2}$  appears which is obtained as the mean square value of cosinus over the angle interval of  $2\pi$ .

After easy but laborious calculations we obtain the following formulae for the frequency spread caused by the presence of the air section  $A_1$  only: for the configuration from Fig. 5a

$$\sigma(f)_t = \frac{n_w f \sigma_1(\alpha)}{\sqrt{2D}} \frac{R_1 - \frac{1}{2}L_1}{R_1 + R_2 - D + (L_{w1} + L_{w2})N} \times \\ \times \left| (R_2 + L_1 - D)n_{a1} + (R_2 - L_2)n_{a2} - \right. \\ \left. - (2R_2 + L_1 - L_2 - D)n_p + (L_{w1} + L_{w2})[N(n_{a1} - 1) - \right. \\ \left. - P(n_p - 1)] + 2L_{w2}(P - N)(n_p - 1) \right| \quad (25)$$

for the configuration from Fig. 5b

$$\sigma(f)_t = \frac{n_w f \sigma_1(\alpha)}{\sqrt{2D}} \frac{R_1 - \frac{1}{2}L_1}{R_1 + R_2 - D + (L_{w1} + L_{w2})N} \times \\ \times \left| (R_2 + L_1 - D)n_{a1} - (R_2 - L_2)n_{a2} + \right. \\ \left. + (D - L_1 - L_2)n_p + (L_{w1} + L_{w2})[N(n_{a1} - 1) - P(n_p - 1)] \right| \quad (26)$$

where

$$N = \frac{2n_w^4 - n_w^2 - 1}{n_w^4 \sqrt{1 + n_w^2}}, \quad (27)$$

$$P = \frac{2}{\sqrt{1 + n_w^2}}, \quad (28)$$

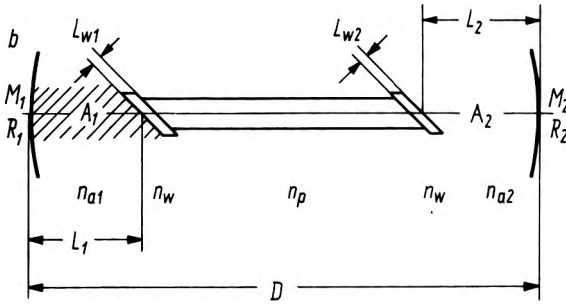
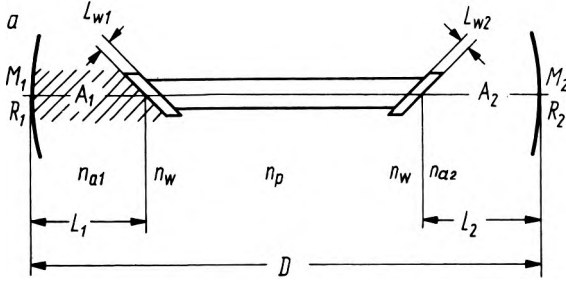


Fig. 5. The two configurations of laser cavity basic for the discussion of the transverse effect caused by one air gap only. The origin of disturbance (air gap  $A_1$ ) shown shadowed. Mirrors  $M_1, M_2$  of the radii  $R_1, R_2$ . Optical windows of thickness  $L_{w1}, L_{w2}$ . Air gaps  $A_1, A_2$  of length  $L_1, L_2$ . Cavity length  $D$ .  $n_{a1}, n_{a2}, n_w, n_p$  — refractive indices of air sections  $A_1, A_2$ , optical windows and plasma section, respectively

$\sigma_1(a)$  denotes the standard deviation of the deflection angle introduced by the air section  $A_1$  only. The remaining notations are explained in Fig. 5. It must be noted that in the present formulae  $n_{a1}, n_{a2}, n_p$  and  $n_w$  are the *actual* values of the refractive indices and *not* the reference values for the standard conditions which we marked previously by the subscript "o" (see eqs. 12, 14, 15 and 20).

The formulae (25) and (26) make possible the computation of a number of special cases. Assuming  $R_1 = \infty$  or  $R_2 = \infty$  we can calculate  $\sigma(f)_t$  in the cases of a plane-spherical cavity (Figs. 6a–d). Assuming  $L_{w2} = 0$  and  $n_{a2} = n_p$  we obtain the cases of a laser with one external and one internal mirror (Figs. 7a–c).

In most practical cases of lasers from Fig. 5 the cavity and configuration is symmetrical

$$n_{a1} = n_{a2} = n_a; \quad L_{w1} = L_{w2} = L_w; \quad R_1 = R_2 = R. \quad (29)$$

We then find:

for the laser from Fig. 5a

$$\sigma(f)_t = \frac{n_w f \sigma_1(a)}{\sqrt{2D}} \frac{R - \frac{1}{2}L_1}{2R - D + 2L_w N} \times \\ \times (2R + L_1 - L_2 - D + 2L_w N)(n_a - n_p), \quad (30)$$

for the laser from Fig. 5b

$$\sigma(f)_t = \frac{n_w f \sigma_1(a)}{\sqrt{2D}} \frac{R - \frac{1}{2}L_1}{2R - D + 2L_w N} \times \\ \times [(D - L_1 - L_2 - 2L_w N)(n_a - n_p) + 2L_w(P - N)(n_p - 1)]. \quad (31)$$

In the practical cases of the plane-spherical cavities from Fig. 6 we may put

$$n_{a1} = n_{a2} = n_a; \quad L_{w1} = L_{w2} = L_w. \quad (32)$$

We then have:

for the laser from Fig. 6a,  $R_1 = \infty, R_2 = R$

$$\sigma(f)_t = \frac{n_w f \sigma_1(a)}{\sqrt{2D}} (2R + L_1 - L_2 - D + 2L_w N)(n_a - n_p); \quad (33)$$

for the laser from Fig. 6b,  $R_1 = R, R_2 = \infty$

$$\sigma(f)_t = \frac{n_w f \sigma_1(a)}{\sqrt{2D}} (2R - L_1)(n_a - n_p); \quad (34)$$

for the laser from Fig. 6c,  $R_1 = \infty, R_2 = R$

$$\sigma(f)_t = \frac{n_w f \sigma_1(a)}{\sqrt{2D}} [(D - L_1 - L_2 - 2L_w N)(n_a - n_p) + \\ + 2L_w(P - N)(n_p - 1)]; \quad (35)$$

for the laser from Fig. 6d,  $R_1 = R, R_2 = \infty$

$$\sigma(f)_t = 0. \quad (36)$$

For the lasers from Fig. 7 with one external and one internal mirror we may put

$$n_{a1} = n_a; \quad L_{w1} = L_w. \quad (37)$$

We then obtain:

for the laser from Fig. 7a in the case of a symmetrical cavity ( $R_1 = R_2 = R$ )

$$\sigma(f)_t = \frac{n_w f \sigma_1(a)}{\sqrt{2D}} \frac{R - \frac{1}{2}L_1}{2R - D + L_w N} \times \\ \times |(R + L_1 - D + L_w N)(n_a - n_p) - L_w(P - N)(n_p - 1)| \quad (38)$$



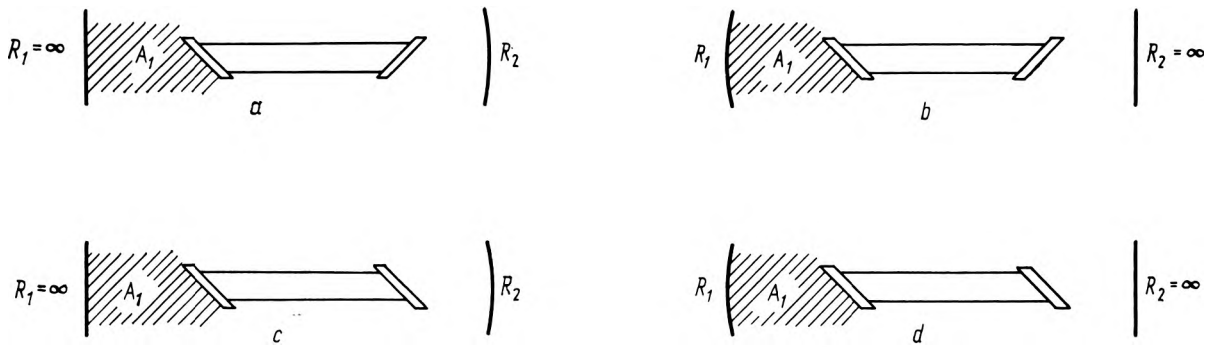


Fig. 6. The four typical cases of a plane-spherical cavity with external mirrors

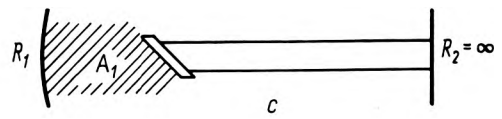
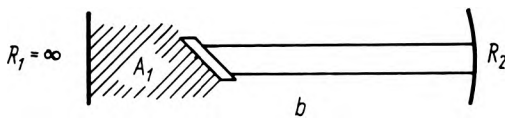
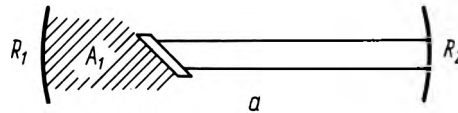


Fig. 7. The three typical cases of a cavity with one internal and one external mirror

for the laser from Fig. 7b,  $R_1 = \infty$ ,  $R_2 = R$

$$\sigma(f)_t = \frac{n_w f \sigma_1(a)}{\sqrt{2D}} \times | (R+L_1-D+L_w N)(n_a-n_p) - L_w(P-N)(n_p-1) |, \quad (39)$$

for the laser from Fig. 7c,  $R_1 = R$ ,  $R_2 = \infty$

$$\sigma(f)_t = \frac{n_w f \sigma_1(a)}{\sqrt{2D}} (R - \frac{1}{2}L_1)(n_a - n_p). \quad (40)$$

In most practical cases some of the formulae (25) through (39) may be simplified by omitting the very small  $(n_p - 1)$ -term.

As follows from the preceding formulae the transverse effect is markedly different for the two possible window arrangements as shown in Fig. 5a and 5b. The effect depends also strongly on the cavity geometry. For instance, a very small transverse effect should be found with a near-confocal cavity from Fig. 7a. On the other hand especially large effects should exhibit the near-concentric cavities from Figs. 5b and 7a as well as long-radius cavities from Figs. 5a and 7. By a proper choice of cavity geometry it is thus in principle possible to minimize the magnitude of the transverse effect. However, in view of the unavoidable simultaneous presence of

the longitudinal effect the formulae rather indicate which cavity types are to be avoided.

When considering the preceding formulae it should be remembered that they represent the influence of one air gap only (air gap  $A_1$ ). To obtain the final magnitude of the effect the influence of each air gap must be calculated separately and then the results added according to the rules for independent random phenomena.

Table 4

Total transverse frequency spread connected with the presence of the air gaps

Laser	Cavity configuration according to Fig.	$\sigma(f)_t$ [Hz]	$\sigma(f)_t/f$
He-Ne	5a(a)	158	$3.3 \times 10^{-13}$
	5b(a)	27	$5.6 \times 10^{-14}$
	7a(b)	46	$9.7 \times 10^{-14}$
CO <sub>2</sub>	7a(c)	$2.9 \times 10^{-2}$	$1.0 \times 10^{-15}$

(a) A single-mode He-Ne laser  $0.63 \mu\text{m}$ . Cavity length  $D = 14 \text{ cm}$ . Mirror radii  $R_1 = R_2 = 40 \text{ cm}$ . Fused silica optical windows,  $L_{w1} = L_{w2} = 5 \text{ mm}$ . Two air gaps,  $L_1 = L_2 = 1 \text{ cm}$ . Laser tube as (a) from Table 1. The total effect caused by both air gaps is given.

(b) Similar laser as (a) except that there is only one air gap of length  $L_1 = 1 \text{ cm}$ .

(c) A low power CO<sub>2</sub> laser. Cavity length  $D = 50 \text{ cm}$ . Mirror radii  $R_1 = R_2 = 60 \text{ cm}$ . Optical window: NaCl,  $L_w = 5 \text{ mm}$ . One air gap of length  $L_2 = 5 \text{ cm}$ . Laser tube as (b) from Table 1.

In order to illustrate the obtained results the total transverse frequency spread due to the presence of the air gaps has been calculated for some characteristic examples. The results are summarized in Table 4.

## 5. The Influence of Dispersive Optical Elements on the Magnitude of the Transverse Effect

In order to improve the frequency selectivity the cavities may be equipped with dispersive elements such as prisms or diffraction gratings (Fig. 8).

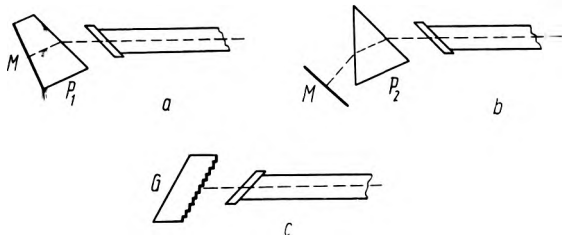


Fig. 8. Dispersive optical elements within a laser cavity (schematically)  
 $M$  — plane mirror;  $P_1, P_2$  — Littrow prisms;  $G$  — blazed diffraction grating

At the first glance it seems that in such cases the lateral movement of the optical axis caused by the transverse effect should produce very large additional change of the optical length of the cavity. However, a closer examination shows this effect to be null. In the case of the Littrow prisms the change of the optical path length within the glass medium is exactly compensated by the reverse change of the optical path length within the air. In the case of a blazed diffraction grating the equiphase surfaces, which are perpendicular to the cavity axis, remain in a fixed relation to the stepped grating surface. Thus, the blazed diffraction grating, in fact, is equivalent to a plane mirror oriented perpendicularly to the cavity axis and not to an inclined reflecting surface.

As a consequence, the presence of the dispersive optical elements does not introduce any additional increase of the transverse effect.

## 6. Frequency Modulation of Gas Lasers Due to Acoustically Induced Gas Density Fluctuations

The preceding sections have been devoted to the discussion of frequency instability due to the statistical fluctuations of gas density. Now we shall

consider similar effects caused this time by the influence of gas density fluctuations accompanying an acoustic interference. In view of a complex geometrical structure of a laser generator with its spacers, mirror mounts, thermal shields and casing we are faced here with a hopelessly complex acoustic diffraction problem. Therefore, we shall only try to estimate the order of effects. To this purpose we shall assume that within the laser cavity there propagates a plane acoustic wave. We shall evaluate the frequency modulation of the laser output connected with the gas density fluctuations and shall not consider the other effects which an acoustic interference can bring about such as the vibrations of the cavity end plates [10, 11] and of the laser tube.

The distribution of acoustic pressure  $p_a$  of a plane acoustic wave propagating in the direction of the  $\xi$ -axis is described by

$$p_a = p_{am} \exp[i(\omega_a t - k_a \xi)], \quad (41)$$

where  $p_{am}$  is the amplitude of acoustic pressure,  $\omega_a$  — acoustic angular frequency,  $k_a$  — wave constant of the acoustic wave. The fluctuations of the pressure cause corresponding fluctuations of gas density and, as a consequence, of its refractive index. From the optical point of view the gaseous medium becomes inhomogeneous and nonstationary. However, as follows from the discussion of the cutoff frequency  $f/2Q$  in Sect. 2.1, for acoustic frequency  $f_a$  we always have  $f_a \ll f/2Q$ . Consequently, the present problem is rigorously quasi-stationary and we may use all previous results.

The acoustic wave may be considered as an adiabatic process. From Poisson equation for adiabatic processes, equation of state for a perfect gas and eqs. (20) and (41) we can calculate the changes of the refractive index of the gas ( $\Delta n$ ) corresponding to alternating acoustic pressure

$$\Delta n = \frac{c_v}{c_p} \frac{n_0 - 1}{p_0} \frac{T_0}{T} p_{am} \exp[i(\omega_a t - k_a \xi)], \quad (42)$$

where  $c_v$  and  $c_p$  is specific heat of the gas at a constant volume and a constant pressure, respectively.

The propagation of a laser beam through a gas subject to acoustic interference may be analyzed in the same manner as in Sect. 2.1. As before, also in the present case we find two effects: the *longitudinal* effect consisting in the change of the optical path length of the undeformed beam, and the *transverse* effect connected with the bending and lateral displacement of the beam. The magnitude of these effects depends on the geometrical length  $L$  of the disturbed optical path and the angle between the direction of propagation of light and sound. In some cases this angular

dependence may produce a partial or even complete cancellation of the effect, for instance, when changes of  $n$  integrated along one section of the path are compensated by opposite and equal changes along the rest of the path etc.

The spatial periodicity of the distribution (42) is equal to the acoustic wavelength  $\lambda_a$ . When  $L \ll \lambda_a$ , i. e. at not too high acoustic frequencies and for not too large  $L$ , the whole considered section of the light beam path will at each moment show a practically constant refractive index irrespective of the direction of the sound wave. In such a case the longitudinal effect will be practically independent of the direction of the interfering acoustic wave. For larger  $L$  and higher frequencies  $f_a$  the longitudinal effect will be the largest when acoustic wave propagates perpendicularly to the laser beam. At other angles the effect will be smaller due to the variations of  $\Delta n$  along the light path.

The transverse effect will be large when the changes of the optical path length across the cross-section of the laser beam are rapid. As a consequence, the effect will be the largest when acoustic wave propagates perpendicularly to the laser beam. For oblique incidence the effect will be smaller or much smaller depending on the angle and relation between  $L$  and  $\lambda_a$ . The effect disappears completely in the case when directions of light and sound are parallel or antiparallel, irrespective of  $L$ .

In order to estimate the magnitude of the effects we shall consider the cases when they are the most pronounced. Thus, according to the preceding discussion we shall assume that the acoustic wave propagates perpendicularly to the cavity axis. Along each light ray the refractive index is then constant at a given moment and in order to calculate the change of the optical path  $\Delta l$  it is only necessary to multiply  $\Delta n$  by the geometrical length  $L$  of the considered section. Placing the point  $\xi = 0$  at the cavity axis we may expand  $\Delta l$  in series around  $\xi = 0$ . We then obtain a similar formula as eqs. (5) and (7)

$$\Delta l(\xi, t) = p_{\text{am}} L \frac{c_v}{c_p} \frac{n_0 - 1}{p_0} \frac{T_0}{T} (1 - i2\pi\xi/\lambda_a) \exp(i\omega_a t). \quad (43)$$

The first term of (43) describes the longitudinal effect. Denoting the amplitude of this effect by  $(\Delta l_0)_m$  we have

$$(\Delta l_0)_m = (n_0 - 1) \frac{c_v}{c_p} \frac{T_0}{T} \frac{p_{\text{am}}}{p_0} L. \quad (44)$$

The transverse effect depends on the tilt angle  $\alpha$  of the equiphase surfaces. The angle  $\alpha$  is obtained by dividing the second term of (43) by the distance

from the axis, i. e. by  $\xi$ . The amplitude of the tilt angle is thus

$$(\alpha)_m = 2\pi(\Delta l_0)_m/\lambda_a. \quad (45)$$

In order to illustrate the presented discussion the results of calculations for some characteristic cases have been summarized in Table 5. In Table 5 only the influence of the air sections has been taken into account. The contributions from the plasma sections have been left out of consideration as they are much smaller due to the comparatively small plasma pressure and large acoustic mismatch existing between the air and the walls of the laser tube. As a consequence, the acoustic wave is reflected effectively at the boundary surface of the laser tube and the plasma column is well screened from acoustic interference.

The effective acoustic pressure of the interfering acoustic wave in Table 5 corresponds to low level speech intensity. At the audibility threshold the

Table 5.

Change of the optical length and bending of the optical axis caused by an interfering acoustic wave traversing a single air gap of the length  $L_a$

	$f_a$ [Hz]	He-Ne laser $L_a = 1$ cm	CO <sub>2</sub> laser $L_a = 5$ cm
$(\Delta l_0)_m$ [m]	any	$1.4 \times 10^{-13}$	$6.7 \times 10^{-13}$
$(\alpha)_m$ [rd]	$10^3$	$2.5 \times 10^{-12}$	$1.2 \times 10^{-11}$

The same lasers as in Table 1. Acoustic wave incident at right angle to the cavity axis. Effective acoustic pressure  $p_{a,\text{eff}} = p_{\text{am}}/\sqrt{2} = 5 \times 10^{-3}$  N/m<sup>2</sup>.

acoustic pressure is approximately one or two orders of magnitude smaller, depending on frequency;  $(\Delta l_0)_m$  and  $(\alpha)_m$  would then be reduced by the same factor.

The frequency modulation of laser light due to acoustic interference may be calculated from formulae of Sect. 3 and 4. As the starting relations are linear in  $\Delta l_0$  and  $\alpha$  this shows that the laser output is frequency modulated at the acoustic frequency  $f_a$ . Replacing in eqs. (22) and (25) through (40)  $\Delta l_0$  by  $(\Delta l_0)_m$  and  $\sigma(\alpha)$  by  $(\alpha)_m$  we get the amplitude of the frequency change, i. e. the maximum value of the frequency deviation:  $(\Delta f_1)_m$  in the case of the longitudinal effect and  $(\Delta f_t)_m$  in the case of the transverse effect.

As follows from the comparison of Table 5 with Table 1 and from inspection of Tables 3 and 4 the magnitude of the acoustic frequency modulation may be surprisingly large in the case of the longitudinal effect. The transverse effect at low and medium acoustic frequencies is much smaller. It could be

more intense at higher frequencies but acoustic interference at these frequencies is generally very weak.

## 7. Conclusions

As follows from the presented discussion the fluctuations of gas density within the cavity may be a source of comparatively large frequency instability, much in excess of the Schawlow-Townes frequency spread  $\Delta f_{sp}$  or the thermally induced frequency spread  $\Delta f_{th}$  as quoted in Sect. 1. These density effects may be of considerable importance when trying to construct the ultra-stable optical frequency standards.

The estimates from Sect. 6 show that it is of great importance to protect the laser effectively from acoustic interference. Most probably this should not present special difficulties.

As regards the influence of statistical fluctuations of gas density the main source of disturbance are the air gaps. The influence of plasma sections is very small or completely negligible.

Surprisingly great values of frequency spread have been found in the case of a short single-mode He-Ne laser. However, due to a small cavity length this in a sense is an extreme case. For longer lasers the frequency scatter would be much smaller due to the increase in both  $D$  and  $r$ . This is readily demonstrated by the example of a CO<sub>2</sub> laser shown in the tables, although of considerable importance there also has been the markedly different cavity type of the CO<sub>2</sub> laser.

As follows from the discussion and the examples the geometry of the cavity can be of large influence. By a proper choice of the cavity type and optical window arrangement and by using short air gaps it should be possible to reduce the magnitude of the frequency spread considerably. The radical elimination of the discussed statistical frequency instability could be achieved by using lasers with internal mirrors or by reducing air pressure within the air gaps.

### L'influence des fluctuations de la densité du gaz sur la stabilité de la fréquence des lasers à gaz

Les fluctuations statistiques de la densité du gaz à l'intérieur du résonateur du laser à gaz changent la longueur optique du résonateur et conduit à la déformation et au déplacement latéral de l'axe optique. On calcule pour les configurations typiques la dispersion de la fréquence causée par ces effets. On montre que la source principale de l'instabilité de la fréquence sont les parties d'air qui se trouvent entre le

tube du laser et les miroirs; les fluctuations statistiques dans le volume de la colonne de la décharge ont une moindre importance. La grandeur de l'effet dépend de la géométrie du résonateur; l'effet peut aggraver l'atteinte finale de la stabilité de la fréquence de l'ultra-stable laser. La façon théorique de l'analyse des phénomènes élaboré dans le travail a été ensuite utilisé pour estimer l'influence de la perturbation acoustique. L'analyse de ce phénomène a démontré qu'elle peut également introduire une considérable instabilité de la fréquence. À la fin ont été proposées les méthodes conduisant à la réduction des fluctuations de la fréquence discutées dans l'article.

### Влияние флуктуации плотности газа на постоянство частоты газовых лазеров

Статистические флуктуации плотности газа в пределах резонатора газового лазера изменяют оптическую длину резонатора и ведут к деформации и бокового смещения оптической оси. В работе вычисляется рассеивание частоты, вызванное этими эффектами для типовых конфигураций. Показано, что главным источником непостоянства частоты являются воздушные промежутки между трубой лазера и зеркалами; статистические флуктуации в пределах колонны лазера имеют меньшее значение. Величина эффекта зависит от геометрии резонатора; эффект может понизить конечное достижимое постоянство частоты ультрастабильного лазерного генератора. Разработанный способ теоретического анализа явлений применяли затем для определения акустической интерференции. Анализ этого явления показал, что и оно может ввести значительное непостоянство частоты. В заключении предлагаются методы уменьшения обсуждаемых флуктуаций частоты.

## References

- [1] SCHAWLOW A. L., and TOWNES C. H., *Infrared and optical masers*, Phys. Rev., **112**, 1940–1949, 1958.
- [2] JASEJA T. S., JAVAN A., MURRAY J., and TOWNES C. H., *Test of special relativity or of the isotropy of space by use of infrared masers*, Phys. Rev., **133**, A1221–A1225, 1964.
- [3] UCHIDA T., *Dynamic behavior of gas lasers*, IEEE J. Quantum Electronics, **QE-3**, 7–16, 1967.
- [4] WOLKENSTEIN M. W., *Molecular optics*, GITTL, Moscow–Leningrad 1951 (in Russian).
- [5] OLIVER B. M., *Thermal and quantum noise*, Proc. IEEE, **53**, 436–454, 1965.
- [6] KOGELNIK H., LI T., *Laser beams and resonators*, Proc. IEEE, **54**, 1312–1329, 1966.
- [7] MAITLAND A., DUNN M. H., *Laser physics*, North Holland Publ. Co., Amsterdam–London 1969.
- [8] KOLOSOVSKY O. A., *The refractive index of the plasma of a CO<sub>2</sub> laser*, Kvantovaya Elektronika, edited by N. G. Basov, Moscow, Sov. Radio, (in Russian) No. 4, 107–109, 1971.
- [9] CARBONE R. J., *Characteristics of a single-frequency sealed-off CO<sub>2</sub> amplifier*, IEEE J. Quantum Electronics, **QE-5**, 48–49, 1969.
- [10] NAGAI H., *Laser frequency fluctuations due to acoustic noise*, Jap. J. Appl. Phys. **11**, 410, 1972.
- [11] NAGAI H., *Laser frequency fluctuations due to mechanical vibrations*, IEEE J. Quantum Electronics, **QE-8**, 857–865, 1972.

Received, October 4, 1973